

Full Length Research Paper

Adaptive trajectory control and friction compensation of a flexible-link robot

Vahid Erfanian* and Mansour Kabganian

Department of Mechanical Engineering, Amirkabir University of Technology, 424, Hafez Ave., Tehran, Iran.

Accepted 10 March, 2009

An adaptive trajectory-tracking controller is developed for a single flexible-link manipulator with presence of friction in the joint and parametric uncertainties. The distributed-parameter dynamic modeling approach is used to design the controller. To eliminate large steady-state tracking error, an adaptive friction compensation technique is proposed based on general static friction model. Reduction of effects of data corruption by noise is obtained using a filtering technique. The global asymptotic stability is guaranteed using the Lyapunov stability theorem. The position tracking performance and link vibration attenuation is verified through experimental results. It also shows that the steady-state joint error is significantly eliminated and the noise effect in the control signal is efficiently reduced.

Key words: Flexible robotic arm, adaptive control, friction compensation, distributed parameter, dual observer.

INTRODUCTION

Power consumption is an important criterion in several industrial applications and this leads to use of lightweight robot manipulators. In addition, reducing the weight of the manipulators makes it possible to achieve lower manufacturing costs, better response times and improved energy efficiency. However, lightweight manipulators tend to be flexible. For instance, in satellites, lightweight robots are desirable and they may be used to carry heavy payloads.

Furthermore, with the increasing demand of fast and accurate control of force and position, compensation of nonlinearities which are inherent in mechanical systems has gain more interest. Most positioning systems, often accompanied by substantial link flexibility, are subjected to nonlinear friction and hence, require advanced frictional compensation. Modeling and compensation of friction is a difficult task for precise motion control of robotic manipulators and it would be even more difficult when a robot has flexible arms. However, controlling flexible arms is a theoretically challenging problem and compensating effects of friction; in a controller this has practical ramifications.

Major approaches to control flexible-link manipulators can be classified into two categories: discretized and distributed-parameter modeling schemes. Many controllers have been constructed based on discretized dynamic modeling approach where the dynamics of flexible link is approximated by a set of finite dimensional equations (that is ordinary differential equations). This approximation technique facilitates the application of finite dimensional control strategies. A robust sliding mode observer was developed in (Chalhoub and Kfoury, 2005) that estimates state variables of the system. In (Knani, 2002) a robust control was designed for flexible mechanisms by a deterministic approach. An observer-based inverse dynamic control strategy was proposed in (Moallem et al., 2001) maintaining robust closed-loop performance. In (Tso et al., 2003) a controller was proposed based on an optical sensing system to measure the flexible link deflection to damp out the tip oscillations and regulate the endpoint of the flexible robot. In fact, discretized methods are with some problems. Due to neglected high frequency dynamics, spillover may occur in the control and observation. To increase accuracy, higher order controllers of a model with more flexible modes are used and from an engineering point of view, these controllers might be difficult to implement since full state measurement or observation are often required.

Due to the flexibility, the system described by finite di-

*Corresponding author. E-mail: erfanian@aut.ac.ir. Tel: +98-2164543456. Fax: +98-21-66419736.

mensional equations (that is partial differential equations) in the second approach is actually a distributed-parameter system. Despite the complexities, this approach is free from spillover problem and many research efforts have been addressed. A model-based control law was designed in (Queiroz et al., 1999) that comprise a distributed-parameter and dynamic boundary equations. In (Zhang et al., 2005) a partial differential equation model was used to design a controller for a nonlinear infinite dimensional system consisting of a flexible two-link manipulator. A moment-feedback trajectory-tracking control for a single flexible link robot was proposed in (Lee, 2004). An outstanding research was performed in (Lee and Prevost, 2005), where a coupled sliding-surface method was proposed for the design of trajectory control of a single flexible link robot. A robust trajectory control scheme was proposed in (Lee and Liang, 2007) for a two-link rigid/flexible robot based on a distributed-parameter dynamic model and a coupled sliding-surface.

Apart from the problem related to the flexibility, friction is an inevitable nonlinear phenomenon in all mechanical systems and the presence of friction turns out to be the main obstacle to achieve good positioning and trajectory-tracking performance. Friction can cause a substantial deterioration of the performance of control. Typical effects are steady-state errors in PD controllers and limit cycles in PID controllers (Olsson et al., 1998). It is well known that steady-state errors of a controlled positioning system can be removed by adding integral actions in the feedback scheme. However, in controlled frictional mechanical systems such integral actions often lead to undesirable stick-slip behavior. Specifically, failing to compensate the friction may cause large tracking errors and oscillations in low speed or velocity reversal conditions. Therefore, high performance tracking control of flexible-link robots cannot be achieved if friction compensation is not properly taken into consideration. In (Lee 2004), it is acknowledged that the steady-state joint tracking errors cannot be reduced to zero due to the friction inside the joint. Accordingly, the steady-state torque of the motor is not zero while it is not rotating. This trouble is noticeably evident in (Tso et al., 2003; Zhang et al., 2005; Lee and Prevost, 2005; Lee and Liang, 2007) where the large steady-state error and non-zero steady-state motor torque still exist.

Friction is a problematical phenomenon to model because it is difficult to describe by a single general model. Many models have been proposed to capture some characteristics of the friction. Those models can be classified as: static models and dynamic models [10]. A static friction model gives a static map between position, velocity and frictional force, whereas a dynamic frictional model gives a dynamics relation between velocity and frictional force, that is, it has an internal state which describes the dynamics of the friction. Dynamic frictional models give a better description of the frictional phenomenon at low velocities, especially when crossing zero velocity. The LuGre

model is a standard dynamic frictional model presented in (Canudas de Wit et al., 1995) that is used in several studies. Despite the complexity of the dynamical frictional models, several simple static frictional models are usually adopted. For example Coulomb-viscous model is by far the most popular and common one. Other models may incorporate the Stribeck effect additionally to do so as well at low velocity. Finally, more complete models are so-called general models that include previous ones as especial cases. In (Ge et al. 2001), a general model-based frictional compensation technique is used to investigate adaptive frictional compensation.

On the other hand, unavoidable noise in control process deteriorates behavior of the system because it influences the actuator driving the joint. This usually increases the bandwidth of the torque control loop and may excite high vibration modes of the flexible-link robot. Moreover, the transient performance is limited because the noise is also amplified in the control process. Consequent ramifications are evidenced in (Tso et al., 2003; Lee, 2004; Lee and Prevost, 2005; Lee and Liang, 2007). A filtering technique is introduced in (Alonge et al., 2007) for rigid robotic manipulators which can be extended for trajectory tracking of flexible-link arms.

In this paper, using particular advantages of the distributed-parameter modeling scheme, an adaptive trajectory-tracking controller is proposed for a horizontal flexible-link robot with parametric uncertainties. An adaptive friction compensation technique is developed to resolve the problem of large steady-state. To obtain a general solution based on the simple method, a general static friction model is used through the linear parameterization technique. To overcome the problem of data corruption by noise, a filtering technique is proposed. The asymptotic stability proof and convergence of the tracking error and flexible link vibration to zero is given using energy dynamics and a suitable Lyapunov design technique. In addition, experiments were carried out to validate the proposed controllers.

System model

Dynamic model of a flexible robot

A horizontal single flexible-link robot with friction in the joint is illustrated in Figure 1 where X_0Y_0 and X_1Y_1 are the fixed and rotating reference frames, respectively. Variables θ , x and $w(x, t)$ are the joint angle, position along the link and link deflection at x , respectively. The flexible link has total length l , mass per unit length ρ , Young's modulus E , constant moment of inertia I , a hub at one end with moment of inertia J_h and a payload mass

M_p at other end with moment of inertia J_p . The flexible link is assumed to be long and slender. Transverse shear and rotary inertia effects are also neglected. This allows

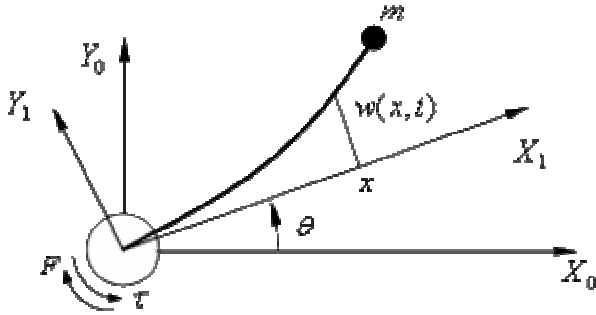


Figure 1. Schematic diagram of a planar flexible-link robot

Bernoulli-Euler beam theory which has infinite number of natural modes of vibration, resulting in an infinite-dimensional dynamic model for the flexible link. The model is as:

$$EIw'''' + \rho(x\ddot{\theta} + \ddot{w}) = 0, \quad 0 < x < l, \quad (1)$$

and the governing equation of motion at the joint is (Lee and Prevost, 2005)

$$J_h \ddot{\theta} - EIw_0'' + F = \tau. \quad (2)$$

For simplification, it is assumed that $\dot{*} = \partial * / \partial t$ and $*' = \partial * / \partial x$. Also, the subscripts 0 and l denote the value of the corresponding variables at $x = 0$ and $x = l$, respectively. F denotes friction torque in the joint, which is described afterwards.

Geometric boundary conditions at $x = 0$ are:

$$w = w' = 0 \quad (3)$$

and the dynamic boundary conditions at $x = l$ are:

$$EIw_l'' = M_p(l\ddot{\theta} + \ddot{w}_l), \quad (4)$$

$$EIw_l''' = -J_p(\ddot{\theta} + \ddot{w}_l'). \quad (5)$$

Frictional modeling

A static frictional model is described by a map between position θ , velocity $\dot{\theta}$ and friction torque F . Hence, the frictional model is defined as $F(\theta, \dot{\theta})$ and described by the general form (Ge et al., 2001):

$$F(\theta, \dot{\theta}) = F_m(\theta, \dot{\theta}) + \varepsilon(\theta, \dot{\theta}), \quad (6)$$

Where ε is the modeling error that is assumed bounded and:

$$F_m(\theta, \dot{\theta}) = \mathbf{S}^T(\theta, \dot{\theta}) \mathbf{p}_f. \quad (7)$$

Equation (7) is linear-in-the-parameters (LIP) model for friction where $\mathbf{S}(\theta, \dot{\theta})$ is a vector of known basis functions and \mathbf{p}_f is the vector of corresponding parameters which is assumed to be unknown but constant. The LIP form, (7), is a more complete presentation and is very desirable for model-based frictional compensation.

Remark 1. A more complete general static frictional model may consist of the following components: stiction, Coulomb, viscous friction torque and Stribeck effect which can be presented as an exponential combination form (Ge et al., 2001):

$$F_m(\theta, \dot{\theta}) = F_C \text{sgn}(\dot{\theta}) + (F_S - F_C) e^{-(\dot{\theta}/\dot{\theta}_s)^2} \text{sgn}(\dot{\theta}) + F_V \dot{\theta}, \quad (8)$$

Where the level of Coulomb frictional coefficient is F_C , F_S is the maximum frictional constant (level of stiction torque) and F_V is the viscous frictional coefficient. The Stribeck effect is represented by the exponential term in (8)

and the empirical parameter $\dot{\theta}_s$ known as Stribeck velocity. This classic model is widely used for uncomplicated and general purpose applications and can approximate the real frictional torque with good precision. Therefore, in this paper, the model expressed by (8) is used as a sample to general frictional static models for experimental verification.

Based on the above discussion, this frictional model can be presented in the LIP form:

$$\mathbf{S}(\theta, \dot{\theta}) = [\text{sgn}(\dot{\theta}) \quad e^{-(\dot{\theta}/\dot{\theta}_s)^2} \text{sgn}(\dot{\theta}) \quad \dot{\theta}]^T, \quad (9)$$

$$\mathbf{p}_f = [F_C \quad F_{SC} \quad F_V]^T, \quad (10)$$

Where $F_{SC} = F_S - F_C$.

Remark 2. Several effects may influence the frictional model. For example, the normal load in the joint may vary due to geometrical conditions changing the friction torque. However, if the structure of the effect is known, it can be simply handled by increasing the space of regressor function and adding the correspondent components.

Assumption 1. The frictional model $F(\theta, \dot{\theta})$ and the regressor vector $\mathbf{S}(\theta, \dot{\theta})$ are assumed bounded for each bounded θ and $\dot{\theta}$

Energy dynamics of the flexible link

payload shown in Figure 1. It can be written as (Lee and Prevost, 2005):

$$E_L = \frac{1}{2} \left[\int_0^l EI w''^2 dx + \int_0^l \rho (\dot{w} + x \dot{\theta})^2 dx + M_p (l \dot{\theta} + \dot{w}_l)^2 + J_p (\dot{\theta} + \dot{w}'_l)^2 \right]. \tag{11}$$

The time rate of the change of E_L is computed as:

$$\dot{E}_L = \left[\int_0^l EI \dot{w}'' \dot{w}'' dx + \int_0^l \rho (\ddot{w} + x \ddot{\theta}) (\dot{w} + x \dot{\theta}) dx + M_p (l \ddot{\theta} + \ddot{w}_l) (l \dot{\theta} + \dot{w}_l) + J_p (\ddot{\theta} + \ddot{w}'_l) (\dot{\theta} + \dot{w}'_l) \right]. \tag{12}$$

Subsequent integration by parts along with the boundary conditions (3)-(5) results in the time derivative of E_L to:

$$\dot{E}_L = -EI w''_0 \dot{\theta}. \tag{13}$$

Remark 3. The total energy of the flexible link and payload defined in (11) and its time rate of change (13) shows that E_L and hence its link of vibration can be reduced asymptotically to zero if $\dot{\theta}$ and $EI w''_0$ are controlled such that $\dot{\theta} = k_m EI w''_0$ with $k_m > 0$, thus resulting in $E_L \geq 0$ and $s = -\dot{\theta} + k_m EI w''_0$. Consequently, the link vibration can be controlled asymptotically to zero if a sliding surface $s = -\dot{\theta} + k_m EI w''_0$ is driven asymptotically to zero (Lee and Prevost, 2005).

Controller design

Considering θ_d as a desired trajectory of θ , the joint-tracking error e is defined as:

$$e = \theta - \theta_d \tag{14}$$

Assumption 2. The desired joint trajectory θ_d and its first and second derivatives, $\dot{\theta}_d$ and $\ddot{\theta}_d$, are assumed to be uniformly bounded. In addition, $\dot{\theta}_d = 0$ and $\ddot{\theta}_d = 0$ are assumed for a period of $t_m \leq t \leq t_f$ with some finite $t_f > t_m > 0$.

By coupling the proportional-integral-derivative, joint-tracking error and the arm bending strain at the joint, the coupled sliding-surface $s(t)$ is defined as:

$$s = (\dot{e} + \Lambda e) + k(e + \Lambda e_I) - k_m EI w''_0, \tag{15}$$

In which e_I is the integration of tracking error defined as:

$$e_I = \int_0^t e dt \tag{16}$$

In (15), k and k_m are positive gains and Λ is a non-negative gain.

Remark 4. The coupled sliding-surface defined in (15) is based on the sliding surface described in Remark 3. Additionally, to accomplish a joint trajectory control, the desired joint velocity $\dot{\theta}_d$, joint-tracking error e , and integrated joint-tracking error e_I were incorporated in the sliding surface.

Additionally, appropriate reference velocity and acceleration signals are defined as:

$$\dot{\theta}_r = \dot{\theta} - s, \tag{17}$$

$$\ddot{\theta}_r = (\ddot{\theta}_d - \Lambda \dot{e}) - k(\dot{e} + \Lambda e) + k_m EI \dot{w}''_0. \tag{18}$$

Based on the definition (15), the sliding-surface dynamics is derived from the joint dynamics (2):

$$J_h \dot{s} = \tau - \mathbf{y}^T \mathbf{p} - \varepsilon, \tag{19}$$

Where the parameter vector \mathbf{p} and the regressor vector \mathbf{y} are defined as:

$$\mathbf{p} = [J_h \quad EI \quad \mathbf{p}_f^T]^T \tag{20}$$

$$\mathbf{y} = [\ddot{\theta}_r \quad -w''_0 \quad \mathbf{S}^T]^T \tag{21}$$

Here a trajectory-tracking control scheme, minimizing the sliding surface asymptotically to zero, is designed based on the distributed-parameter dynamic model, which is described in the following theorem.

Theorem 1. Consider a flexible-link robot presenting friction in the joint where the model of friction is described by (6)-(7) satisfying Assumption 1 and the dynamics of flexible-link is described by (1)-(5) with parametric uncertainties. Suppose that the control objective is to have a flexible-link robot track a desired trajectory under Assumption 2 as accurately as possible while promptly suppressing the resulting link vibration asymptotically to zero and attenuate the influences of data corruption by noise. Then the following control law (22) with adaptations law (23) and filter dynamic (24) can achieve the objective while keeping all internal signals bounded.

$$\tau = \mathbf{y}^T \hat{\mathbf{p}} - k_r \left| EIW_0''(\dot{\theta}_d - \Lambda e) \right| s - \frac{1}{k_m} (\dot{e} + \Lambda e) - k_D \hat{s} - u_r, \quad (22)$$

And

$$\dot{\hat{\mathbf{p}}} = \mathbf{\Gamma} s \mathbf{y}^T (\theta, \dot{\theta}, \ddot{\theta}, \ddot{\theta}_r), \quad (23)$$

where $\hat{\mathbf{p}}$ is the estimation of \mathbf{p} and

$$T \dot{\hat{s}} = s - \hat{s}. \quad (24)$$

In (22), u_r is a robust control term for suppressing any modeling uncertainty that will be explained, subsequently k_r , k_D and T are also positive constant gain. In (23), $\mathbf{\Gamma}$ is a gain matrix correspondent to \mathbf{p} which is assumed to be a positive definite diagonal matrix and is defined as:

$$\mathbf{\Gamma} = \text{diag}(\Gamma_{J_h}, \Gamma_{EI}, \Gamma_f). \quad (25)$$

Where Γ_f a positive definite diagonal gain matrix corresponding to \mathbf{p}_f as well; Γ_{J_h} and Γ_{EI} are positive constant gains.

Remark 5. The proposed control is a filtered PIDS (proportional integral derivative and strain) control with friction compensation and dynamics feed-forward. It is also a collocated trajectory control since the actuator generating τ and the sensors measuring θ and EIW_0'' are all collocated at the joint hub. Consequently, based on the distributed-parameter dynamic model, the proposed control scheme is robust to the spillover instability (Lee and Prevost, 2005).

At this point, to prove the above mentioned theorem, it is convenient to give the following assertion:

Assertion1. Let consider the strictly proper and asymptotically stable linear system (24). If input s is bounded and uniformly continuous, and output $\hat{s} \rightarrow 0$ asymptotically as $t \rightarrow \infty$, then $s \rightarrow \infty$ asymptotically as $t \rightarrow \infty$.

Proof of Assertion 1. If s is bounded then \hat{s} is bounded and uniformly continuous (Slotine and Li, 1991). As s is uniformly continuous, \hat{s} is uniformly continuous. As $\hat{s} \rightarrow 0$ asymptotically as $t \rightarrow \infty$ and \hat{s} is uniformly continuous, using Barbalat lemma, it follows that $\dot{\hat{s}} \rightarrow 0$ asymptotically as $t \rightarrow \infty$ and consequently, $s \rightarrow 0$ asymptotically as $t \rightarrow \infty$.

Proof of Theorem 1. A candidate Lyapunov functional $V(t)$ is considered:

$$V(t) = E_L + \frac{1}{2} J_h s^2 + \frac{1}{2} \frac{k}{k_m} (e + \Lambda e_I)^2 + \frac{1}{2} k_D T \hat{s}^2 + \frac{1}{2} \tilde{\mathbf{p}}^T \mathbf{\Gamma}^{-1} \tilde{\mathbf{p}} \quad (26)$$

Where $\tilde{\mathbf{p}} = \hat{\mathbf{p}} - \mathbf{p}$ is the vector of estimation error of system parameters

Remark 6. The weight of the joint-tracking control $e + \Lambda e_I$ relative to the flexible link energy E_L is described by the ratio k/k_m in $V(t)$. As a consequence, larger values of k/k_m which deals with emphasizing the joint-tracking control, result in faster suppression of the joint-tracking errors. Smaller values of k/k_m stressing the flexible link energy, lead to faster suppression of the link vibration.

The time derivative of the candidate of Lyapunov function (26) is computed as:

$$\dot{V} = -EIW_0'' \dot{\theta} + J_h s \dot{s} + \frac{k}{k_m} (e + \Lambda e_I) (\dot{e} + \Lambda e) + k_D \hat{s} (s - \hat{s}) + \tilde{\mathbf{p}}^T \mathbf{\Gamma}^{-1} \dot{\tilde{\mathbf{p}}}, \quad (27)$$

Where (13) and (24) are used, by substituting sliding-surface dynamics (19) into (27) it follows:

$$\begin{aligned} \dot{V} = & -EIW_0'' \dot{\theta} + s \left\{ \mathbf{y}^T \tilde{\mathbf{p}} - k_r \left| EIW_0''(\dot{\theta}_d - \Lambda e) \right| s - \frac{1}{k_m} (\dot{e} + \Lambda e) - k_D \hat{s} - u_r - \varepsilon \right\} \\ & + \frac{k}{k_m} (e + \Lambda e_I) (\dot{e} + \Lambda e) + k_D s \hat{s} - k_D \hat{s}^2 + \tilde{\mathbf{p}}^T \mathbf{\Gamma}^{-1} \dot{\tilde{\mathbf{p}}}. \end{aligned} \quad (28)$$

Using (15) it follows that:

$$EIW_0'' \dot{\theta} = EIW_0'' (\dot{\theta}_d - \Lambda e) - \frac{1}{k_m} \left[s - (\dot{e} + \Lambda e) - k(e + \Lambda e_I) \right] (\dot{e} + \Lambda e). \quad (29)$$

By substituting (29) and (20)-(21) in (28) it results that:

$$\begin{aligned} \dot{V} \leq & -k_r \left| EIW_0''(\dot{\theta}_d - \Lambda e) \right| \left(s^2 - \frac{1}{k_r} \right) - \frac{1}{k_m} (\dot{e} + \Lambda e)^2 - k_D \hat{s}^2 - s(\varepsilon + u_r) + \\ & + s \left\{ \tilde{J}_h \ddot{\theta}_r - \tilde{E}IW_0'' + S^T(\theta, \dot{\theta})^T \tilde{\mathbf{p}}_f \right\} + \tilde{\mathbf{p}}^T \mathbf{\Gamma}^{-1} \dot{\tilde{\mathbf{p}}}. \end{aligned} \quad (30)$$

Extracting the adaptation laws (23) of system parameters:

$$\dot{\tilde{J}}_h = -\Gamma_{J_h} \ddot{\theta}_r s, \quad (31)$$

$$\dot{EI} = \Gamma_{EI} W_0'' s, \tag{32}$$

$$\dot{\mathbf{p}}_f = -\Gamma_f \mathbf{S}(\theta, \dot{\theta}) s, \tag{33}$$

and inserting (31)-(33) into (30), it outcomes

$$\dot{V} \leq -k_r |EI W_0'' (\dot{\theta}_d - \Lambda e)| \left(s^2 - \frac{1}{k_r} \right) - \frac{1}{k_m} (\dot{e} + \Lambda e)^2 - k_D \hat{s}^2 - s(\varepsilon + u_r). \tag{34}$$

Since the robust term u_r is chosen as:

$$u_r = K_r \text{sgn}(s) \tag{35}$$

Where K_r is a constant gain and $K_r \geq |\varepsilon|$, (34) follows:

$$\dot{V} \leq -k_r |EI W_0'' (\dot{\theta}_d - \Lambda e)| \left(s^2 - \frac{1}{k_r} \right) - \frac{1}{k_m} (\dot{e} + \Lambda e)^2 - k_D \hat{s}^2. \tag{36}$$

then $\dot{V} < 0$ is guaranteed for all $s(t)$ satisfying that $s^2 > 1/k_r$. This implies the boundedness of $V(t)$ and hence the boundedness of variables $s, \hat{s}, (e + \Lambda e_1)$ and E_L involved in (26). Then, $\dot{\hat{s}} \in L_\infty$ follows from filter dynamics (24) with the boundedness of s and \hat{s} . The boundedness of E_L guarantees that of EIW_0'' , and the boundedness of $(e + \Lambda e_1)$ guarantees that of e and e_1 . Then the boundedness of \dot{e}_1 and hence $\dot{\theta}$ follows from the sliding surface (15) with the boundedness of s, e, e_1 , and EIW_0'' . The boundedness of \dot{w} and \dot{w}' follows from that of E_L with the boundedness of $\dot{\theta}$. In addition, the boundedness of \dot{w} and EIW_0'' implies $E\dot{H}W''$. Then, $\dot{s} \in L_\infty$ follows from the sliding surface dynamics (19) and control law (22); $\ddot{e} \in L_\infty$ follows from the joint dynamics (2) and control law (22) since $\ddot{\theta}_d$ is uniformly bounded. Integration of \dot{V} obtained in (36) yields $\hat{s}, \hat{s}, (\dot{e} + \Lambda e) \in L_2$. Since $\hat{s}, \ddot{e}, \dot{e} \in L_\infty$, as a consequence of Barbalat lemma, $\hat{s}, (\dot{e} + \Lambda e) \rightarrow 0$ asymptotically as $t \rightarrow \infty$, which guarantees $\dot{e}, e \rightarrow 0$ asymptotically as $t \rightarrow \infty$. Therefore, Assertion 1 provides $s \rightarrow 0$ from $s \in L_\infty$ and $\hat{s} \rightarrow 0$. Then the definition of the sliding surface (15) yields $k\Lambda e_1 + k_m EIW_0'' \rightarrow 0$ asymptotically as $t \rightarrow \infty$.

vibration to zero in the steady state while $\dot{\theta}_d = 0$ is assumed for time period $t_m \leq t \leq t_f$ with some finite $t_f > t_m > 0$. Since e_1 is bounded and $\dot{e}, e \rightarrow 0$ asymptotically as $t \rightarrow \infty$, e_1 approaches a finite constant, which implies EIW_0'' also approaches a finite constant since $k\Lambda e_1 + k_m EIW_0'' \rightarrow 0$ asymptotically as $t \rightarrow \infty$. When non-zero for a horizontal flexible robot, the link is EIW_0'' , will vibrate and hence oscillate since the joint hub will not rotate in the steady state. Due to existence of structural damping, even neglected, EIW_0'' should be zero for a horizontal flexible robot when EIW_0'' remains constant in the steady state, which implies $e_1 \rightarrow 0$ asymptotically as $t \rightarrow \infty$. Asymptotic stability of EIW_0'' implies that of link deflection w . ■

The above control laws differ from that proposed by (Lee and Prevost, 2005) in the following aspects: (i) the presence of adaptive compensation of general static frictional model, (ii) the PIDS control action is obtained from the output of a low pass filter supplied by s

Remark 7. The presence of the $\text{sgn}(\cdot)$ function in the control inevitably introduces chattering, which is undesirable as it may excite mechanical resonance. To alleviate this problem, many approximation mechanisms have been used, such as boundary layer, saturation functions, and hyperbolic tangent function $\tanh(\cdot)$ which have the following property (Ge et al., 2001):

$$0 \leq |s| - s \tanh\left(\frac{s}{\gamma_1}\right) \leq 0.2785\gamma_1, \quad \forall s \in R \tag{37}$$

By smoothing the $\text{sgn}(\cdot)$ function, the closed-loop system is also stable but with a small residue error. For example, if $u_r = K_r \tanh(s/\gamma_1)$, where $\gamma_1 > 0$ is a constant, then (36) becomes:

$$\dot{V} \leq -k_r |EI W_0'' (\dot{\theta}_d - \Lambda e)| \left(s^2 - \frac{1}{k_r} \right) - \frac{1}{k_m} (\dot{e} + \Lambda e)^2 - k_D \hat{s}^2 + |s| |\varepsilon| - K_r s \tanh\left(\frac{s}{\gamma_1}\right). \tag{38}$$

Using (37) and reconsidering that $K_r \geq |\varepsilon|$, (38) can be further simplified as:

$$\dot{V} \leq -k_r |EI W_0'' (\dot{\theta}_d - \Lambda e)| \left(s^2 - \frac{1}{k_r} \right) - \frac{1}{k_m} (\dot{e} + \Lambda e)^2 - k_D \hat{s}^2 + 0.2785\varepsilon K_r. \tag{39}$$

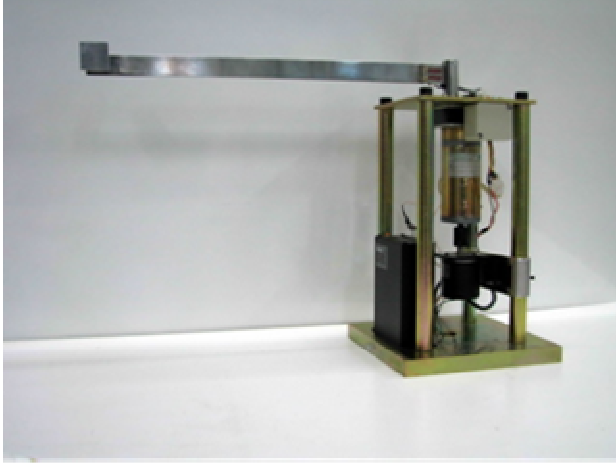


Figure 2. Experimental setup

Obviously, $\dot{V} \leq 0$ whenever the system state variable vector \mathbf{r} is outside the compact set:

$$D = \left\{ \mathbf{r} \mid 0.2785\epsilon K_r \geq k_r |EIw''(\dot{\theta}_d - \Lambda e)| \left(s^2 - \frac{1}{k_r} \right) + \frac{1}{k_m} (\dot{e} + \Lambda e)^2 + k_D s^2 \right\}. \quad (40)$$

Thus, the closed-loop system is stable and tracking error will converge to a small neighborhood of zero, whose size is adjustable by the design parameters K_r and γ_1 . Additionally, to get rid of discontinuity problem in the control law due to compensation of dry friction, the above modification should also be utilized. For instance, the frictional compensation feed forward for the model (7) respect to (9)-(10) is modified as:

$$\hat{F}_m(\theta, \dot{\theta}) = \mathbf{S}_1(\theta, \dot{\theta}) \hat{\mathbf{p}}, \quad (41)$$

Where \mathbf{S}_1 is the modification of \mathbf{S} as:

$$\mathbf{S}_1(\theta, \dot{\theta}) = \begin{bmatrix} \tanh\left(\frac{\dot{\theta}}{\gamma_2}\right) & e^{-(\dot{\theta}/\dot{\theta}_s)^2} \tanh\left(\frac{\dot{\theta}}{\gamma_2}\right) & \dot{\theta} \end{bmatrix}^T, \quad (42)$$

Where $\gamma_2 > 0$ and $\hat{\mathbf{p}}$ is the vector of estimated friction parameters correspondent to (10).

It should be mentioned that these modification may cause the estimated parameters growth. To deal with this problem, other modification schemes can be used to modify the adaptive laws to guarantee the robustness of the closed-loop system in the presence of approximation error (Ge et al., 2001).

Experimental Validation

Now, it is necessary to prove the convergence of link to

evaluate the proposed adaptive control laws and frictional compensation schemes practically, a horizontal flexible-link robot was set up, shown in Figure 2. Experiments have been carried out using a horizontal flexible-link robot and its payload mass consisting of a DC motor equipped with a 400 PPR encoder and driven by the PWM control with a base frequency of 20 kHz. A full-bridge strain gauge is used to measure the bending strain at the neck of the flexible arm through a strain amplifier and an A/D converter, under the assumption of small link deflection. A hardware low-pass filter having a bandwidth of 1 kHz is used to filter the high-frequency noises. A gear-box with the ratio of 1/37 is used. A PC with a Pentium III CPU is used to process data with a sampling period of 1 kHz.

Remark 8. Although the flexible arm is considered as a distributed-parameter system, in practice while verifying the performance of the controllers, it is inevitably some computation and then the amplifier producing a current for the motor has finite bandwidth. Therefore, to reduce the effects of digital computation, the sampling period of data processing is chosen 1 kHz where higher natural frequencies of the flexible arm are comprised. The experimental setup features a flexible arm driven by a permanent magnetic DC motor. The self-inductive effect of the DC motor is neglected. Therefore, a mathematical model for the DC motor torque τ is:

$$\tau = K_T i_a \quad (43)$$

$$E = K_{emf} \dot{\theta} + R i_a, \quad (44)$$

where i_a , K_T , K_{emf} , R and E are motor current, torque constant, back EMF, resistance and input voltage of the DC motor, respectively. Coupling (43) and (44) with equation of motion (2) results in:

$$J_h \ddot{\theta} - EI w_0'' + \dot{F} = \tau^*, \quad (45)$$

Where

$$J_h^* = RK_T^{-1} J_h \quad (46)$$

$$EI^* = RK_T^{-1} EI \quad (47)$$

$$\dot{F}^* = RK_T^{-1} \dot{F} + K_{emf} \dot{\theta}, \quad (48)$$

$$\tau^* = E \quad (49)$$

The obtained equation of motion (45) is identical to its the original (2). The characteristic of EMF is similar to

Table 1. True values of system parameters measures practically

Parameter	True Values	
J_h	0.28	V.s ² .rad ⁻¹
EI	6.50	V.m
F_C	5.47	V
F_{SC}	0.73	V
F_V	0.96	V.s.rad ⁻¹

Table 2. Constant gain

Gain	Value	
Λ	10 ⁻⁷	s ⁻¹
k	5.0	s ⁻¹
k_m	0.87	V ⁻¹ .s ⁻¹ .rad
k_r	55.4	s ² .rad ⁻²
K_r	0.97	V
T	0.01	s
k_D	1.15	V.s.rad ⁻¹
Γ_{EI}	5.87	V.m ² .rad ⁻¹
Γ_{J_h}	6.38×10 ⁻³	V.s ⁴ .rad ⁻³
Γ_{F_C}	11.48	V.rad ⁻¹
$\Gamma_{F_{SC}}$	0.45	V.rad ⁻¹
Γ_{F_V}	1.28	V.s ² .rad ⁻³

viscous friction and hence is considered as a supplementing term to the frictional model. Based on (46)-(49), the true values of the coupled system parameters are practically measured and shown in Table 1. Normal notation is used to show the parameters instead of using star superscription.

The flexible arm was made of spring steel strip with thickness of 1.1mm. The first and second natural frequencies of the flexible link and payload mass are 2.5 and 36.2Hz, respectively. The Stribeck velocity constant was measured $\dot{\theta}_s = 0.1$ rad/s. The modification factors γ_1 and γ_2 are both chosen as 0.01 rad/s. The constant gains are chosen as in Table 2.

To generate the desired signal, the basis function Θ_d is defined:

$$\Theta_d = \begin{cases} 6\left(\frac{t}{t_m}\right)^5 - 15\left(\frac{t}{t_m}\right)^4 + 10\left(\frac{t}{t_m}\right)^3, & 0 \leq t < t_m \\ 1, & t_m \leq t < t_f \end{cases} \quad (50)$$

Where $t_m < t_f$. The following periodic function is chosen for the desired joint trajectory:

$$\theta_d = R \begin{cases} \Theta_a(t-at_f), & a \leq t/t_f < a+1 \\ 1-\Theta_a(t-bt_f), & b \leq t/t_f < b+1 \end{cases} \quad a = 0, 2, 4, K, \quad b = 1, 3, 5, K \quad (51)$$

Where t_m , t_f and R are chosen 2 s, 3 s and $\pi/2$ rad, respectively.

Experiments were carried out with zero initial value for the estimated parameters. Figure 3 shows the experimental results.

The desired joint trajectory angle θ_d and the joint tracking angle θ are shown in Figure 3(a) and the joint tracking error e is shown in Figure 3(b). The test is subject to parameter uncertainty due to zero initial values for estimated parameters. This temporarily increases the tracking error as shown in Figure 3(b), but the tracking error reduces eventually because the frictional and dynamical feed forward terms in the control law are augmented during parameter estimation progression. The estimation of frictional parameters \hat{F}_s , \hat{F}_{SC} and \hat{F}_V are shown in

Figure 3(e) and that of dynamical parameters \hat{J}_h and

\hat{EI} are shown in Figure 3(f). As it is shown, all estimated parameters are bounded. However, due to values of the constant gain Γ , the rate of estimation can be adjusted. The effect of frictional compensation feed forward in the control signal is obvious where the direction of the joint velocity changes. The tracking error approximately converges to zero in local steady-state durations of the desired input and reasonably, this shows achievement to main objective of this paper to eliminate large steady-state tracking errors, Figure 3(b). Reasonably, it shows the proper frictional modeling and compensation technique had been proposed. Consequently, the trouble of existence of large steady-state control signal and tracking error during local stationary desired input signal is resolved. In (Tso et al. 2003; Zhang et al. 2005; Lee 2004; Lee and Prevost 2005; Lee and Liang 2007) because of existence of significant friction in the mechanical system and in absence of appropriate dominative friction compensation they were not able to eliminate the large steady-state motor torque and tracking error.

The bending curvature at neck of flexible arm, w_0'' is shown in Figure 3(d). As it is shown, reduction of bending curvature of flexible arm during transient state denotes satisfactory performance. Particularly, bending curvature during local steady-state desired input converges approximately to zero that implies acceptable link vibration cancellation. It must be realized that the most serious source of inaccuracy in vibration elimination of the flexible arm is due to the backlash in the reducing gearbox. As it was

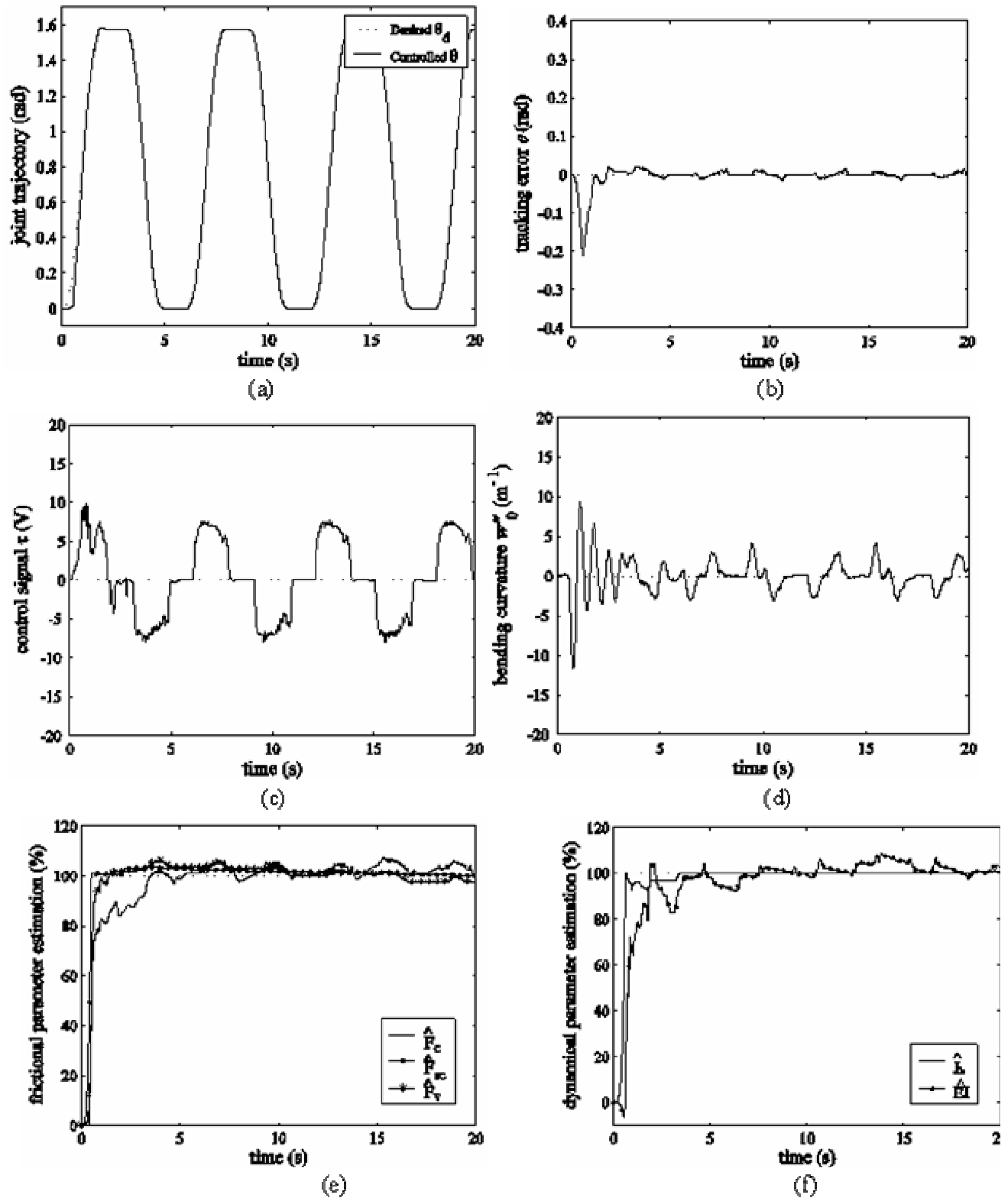


Figure 3. Experimental results. (a) Trajectory tracking. (b) Tracking error. (c) Control signal. (d) Bending curvature of the flexible link. (e) Estimation of frictional parameters. (f) Estimation of dynamical parameters.

mentioned in Remark 6, smaller k/k_m leads to faster link Vibration cancellation. In addition, Figure 3(c) denotes

that the control scheme allows obtaining good behavior, because it is able to attenuate the effects of data corrup-

ted by noise. This signifies reduction of high frequency harmonics of the signals used to generate the control torque gained by \hat{s} .

Conclusion

An adaptive frictional compensation approaches has been theoretically and experimentally investigated for a single flexible-link manipulator. The used of distributed-parameter modeling approach was free from the spillover instability. Experimental results carried out on a flexible-link robot; show that the problem of large steady-state joint tracking error was resolved. It also denoted the proper used general static model of friction. The vibration attenuation of the flexible link during transient and steady state signifies the acceptable performance of the controllers. The effects of noise in data corruption were also reduced by the filtering technique. Finally, as a future study, dynamic frictional models will be researched further to take into consideration the dynamic behavior friction.

REFERENCES

- Alonge F, D'ippolito F, Raimondi FM (2007). A Control Law for Robotic Manipulators Based on a Filtered Signal to Generate PD Action and Velocity Estimates, *Int. J. Robot. Autom.* 22: 2.
- Canudas de WC, Olsson H, Åstrom KJ, Lischinsky P (1995). A New Model for Control of Systems with Friction, *IEEE Trans. Autom. Control*, 40 (3): 419-425.
- Chalhoub NG, Kfoury GA (2005). Development of a Robust Nonlinear Observer for a Single-Link Flexible Manipulator, *Nonlinear Dynamics*, 39: 217-233.
- de Queiroz MS, Dawson DM, Agarwal M, Zhang F (1999). Adaptive Nonlinear Boundary Control of a Flexible Link Robot Arm, *IEEE Trans. Robot. Autom.* 15 (4): 779-787.
- Ge SS, Lee TH, Ren SX (2001). Adaptive Friction Compensation of Servo Mechanisms, *Int. J. Syst. Sci.* 32 (4): 523-532.
- Knani J (2002). Dynamic Modelling of Flexible Robotic Mechanisms and Adaptive Robust Control of Trajectory Computer Simulation—Part I, *Appl. Mathematical Modelling*, 26: 1113-1124.
- Lee HH (2004). A New Trajectory Control of a Flexible link Robot Based on a Distributed-Parameter Dynamic Model, *Int. J. Contr.* 77 (6): 546-553.
- Lee HH, Liang Y (2007). A Coupled-Sliding-Surface Approach for the Robust Trajectory Control of a Horizontal Two-Link Rigid-Flexible Robot, *Int. J. Contr.* 80(12): 1880-1892.
- Lee HH, Prevost J (2005). A Coupled Sliding-Surface Approach for the Trajectory Control of a Flexible link Robot Based on a Distributed Dynamic Model, *Int. J. Contr.* 78 (9): 629-637.
- Moallem M, Patel RV, Khorasani K (2001). Nonlinear Tip-Position Tracking Control of a Flexible link Manipulator: Theory and Experiments, *Automatica*. 37: 1825-1834.
- Olsson H, Åström KJ, Canudas de WC, Gäfvert M, Lischinsky P (1998). Friction Models and Friction Compensations," *Eur. J. Cont.* 4 (3): 176-195.
- Slotine JJE, Li WP (1991). *Applied Nonlinear Control*, New Jersey: Prentice-Hall, pp. 124-125.
- Tso SK, Yang TW, Xu WL, Sunb ZQ (2003). Vibration Control for a Flexible link Robot Arm with Deflection Feedback, *Int. J. Non-Linear Mech.* 38: 51-62.
- Zhang X, Xu W, Nair SS, Chellaboina V (2005). PDE Modeling and Control of a Flexible Two-Link Manipulator, *IEEE Trans. Contr. Syst. Technol.* 13 (2): 301-312.